LANGMUIR

Article

Cationic amphiphiles bearing a diacetylenic function in the headgroup: aggregative properties and polymerization

Alessandro Mauceri, Luisa Giansanti, donatella capitani, anatoly sobolev, Luciano Galantini, Mauro Bassetti, Maria Grazia nemi, Denise Gradella Villalva, Sara Battista, and Giovanna Mancini

Langmuir, **Just Accepted Manuscript** • DOI: 10.1021/acs.langmuir.0c01735 • Publication Date (Web): 24 Sep 2020

Cationic amphiphiles bearing a diacetylenic function in the headgroup: aggregative properties and polymerization

Alessandro Mauceri,[§ †] Luisa Giansanti, [‡] Donatella Capitani,[†] Anatoly Sobolev,[†] Luciano Galantini,[§] Mauro Bassetti,[#] Maria Grazia Nemi,[#] Denise Gradella Villalva,[§ †] Sara Battista, [‡] Giovanna Mancini[†]*

[§]Dipartimento di Chimica, Università di Roma "Sapienza", P.le A. Moro 5, 00185 Roma (Italy); [‡]Dipartimento di Scienze Fisiche e Chimiche, Università degli Studi dell'Aquila, Via Vetoio 10, 67010 Coppito (Italy); [†]CNR - Istituto per i Sistemi Biologici, Via Salaria km 29.300, 00016 Monterotondo Scalo, RM, Italy; [#]CNR, Istituto per i Sistemi Biologici c/o Dipartimento di Chimica, Università di Roma "Sapienza", P.le A. Moro 5, 00185 Roma (Italy).

KEYWORDS chain length; effect of surfactants concentration; Langmuir monolayer; micelle polymerization; polydiacetilenic amphiphile; twin surfactant

ABSTRACT

In the wide panorama of diacetylenic lipids the photo-responsive conjugated 1,3-diyne function is usually encased into the hydrocarbon chain of the amphiphile at variable distance from the headgroup. Therefore, the polydiacetylene network obtained by polymerization upon UV irradiation of the corresponding liposomes, exploited as sensing function, is embedded in the hydrophobic region of liposomes. Structurally related cationic diacetylenic amphiphiles featuring the conjugated triple bonds proximate to charged nitrogen were synthesized and evaluated in their ability to polymerize in aggregative conditions. The occurrence of polymerization only in certain aggregating conditions was rationalized by NMR and Langmuir trough experiments.

INTRODUCTION

Polydiacetylenes (PDAs) are *ene-yne* conjugated polymers formed upon 1,4-photopolymerization by UV or γ-light irradiation of diacetylenes, which only proceeds when diacetylenic molecules are

well aligned and closely packed in ordered structures such as crystal lattices or self-assembled systems.[1,2] In almost fifty years from the first preparation reported by Wegner in 1969,[3] PDAs have been extensively investigated due to their unique optical and structural properties.[4-6] In particular, the capability of PDAs to undergo modifications in their emission and/or absorption spectra upon exposure to certain stimuli such as specific molecular recognition[7-9] or changes in the external conditions such as temperature,[10,11] pH[12] or solvent,[13,14] has designated them as very promising molecular devices for sensor applications.

Diacetylenic amphiphiles constitute an elected class of molecules to obtain PDAs thanks to their ability to self-assemble into molecular films, micelles or vesicles, in which the geometrical requirements for the occurrence of polymerization are satisfied. A wide amount of diacetylenic amphiphiles has been synthesized[15-30] and most of them bear the photo-responsive diacetylenic function encased into the hydrocarbon chain of the amphiphile at variable distance from the head group, whereas few examples of amphiphiles showing the diacetylenic function in proximity of the hydrophilic headgroup have been reported.[28-30]

As mentioned above, polymerization can occur if the diacetylenic units are closely packed, in particular they should be preorganized at a distance *d* that matches the repeat distance of the polymer, *i.e.* 4.9 Å, with C(1)-C(4) distance (*s*) of 3.4 Å and a tilt angle

of 45° (Scheme 1).[2] A position in the middle of hydrophobic chain might favor polymerization; however, efficient packing of hydrophobic chains is not sufficient, per se, to guarantee polymerization since other parameters such as hydrogen bonding between headgroups and the extent of headgroup hindrance are crucial.[30] The occurrence of a high extent of polymerization is reflected by the appearance of a variety of colors, from deep blue to orange. The most fascinating feature of PDAs is their above mentioned chromism in response to external stimuli, in particular their blue to red color transition associated with a change in their backbone conformation from planar to non planar. The colorimetric response strongly depends on the position of the ene-yne backbone along the hydrophobic chain, and it was observed stronger when the polymeric chromophore is close to the headgroups.[30] The minor response of the ene-yne backbone to external stimuli in correspondence of a deeper positioning along the hydrophobic chain was attributed to a cohesive energy of the alkyl chain between the diacetylene group and the headgroup.[30]

Hence, it is evident that the placement of polymerizable residues close to the headgroups is a delicate issue that requires molecular structures addressing a compromise between topological conditions guaranteeing, on the one hand, polymerization and, on the other, a high chromatic response.

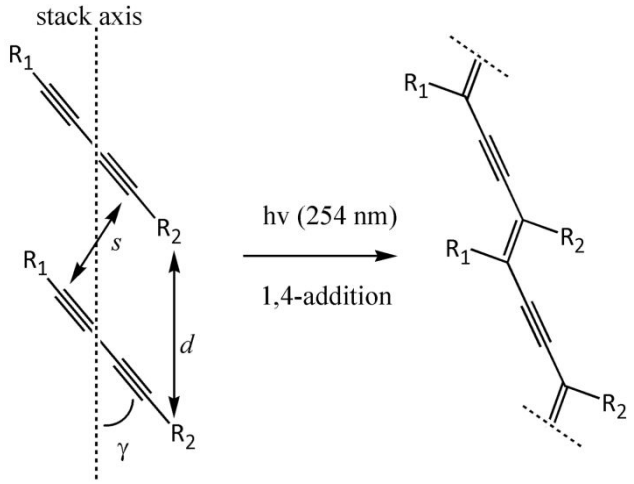

Scheme 1. Favourable geometric parameters of monomers in crystal lattice (d = 4.9 Å, s = 3.4 Å, γ ~ 45 °) for topochemical polymerization.

Here we report on the synthesis and the physicochemical characterization of three structure-analogues cationic diacetylenic amphiphiles (CDs) **1**, **2** and **3** (Chart 1), characterized by an unprecedented molecular structure in which the diacetylenic moiety is not included in the hydrocarbon chain but embedded between two hydrophilic groups, *i.e.* a quaternary nitrogen and a hydroxyl group. Besides the structural analogues CDs **1-3**, constituted by a hydroxyhexadiynyl moiety linked to the ammonium head group and a hydrophobic chain of different length (*i.e.* C16, C18 and C20), another novel amphiphile bearing the diacetylenic function included in one of the two hydrophobic chains, CD **4**, in analogous proximity to the charged nitrogen, was synthesized, for comparison with CDs **1-3**. The aggregative properties of CDs **1-4** in

aqueous solution were investigated and their capability to polymerize was ascertained by UV-vis and ^{1}H-NMR spectroscopies. Furthermore, surface pressure-area isotherm analysis of Langmuir monolayers formed by CDs **1-3** was performed and compared to that of two cationic surfactants, *i.e.* *N*-hexadecyl-*N*,*N*,*N*-trimethylammonium bromide (CTAB) and cetyl-*N*-(2-hydroxyethyl)-*N*,*N*-dimethylammonium bromide (CDHB), with the purpose to obtain additional information on the organization of the aggregates formed by the newly synthetized amphiphiles.

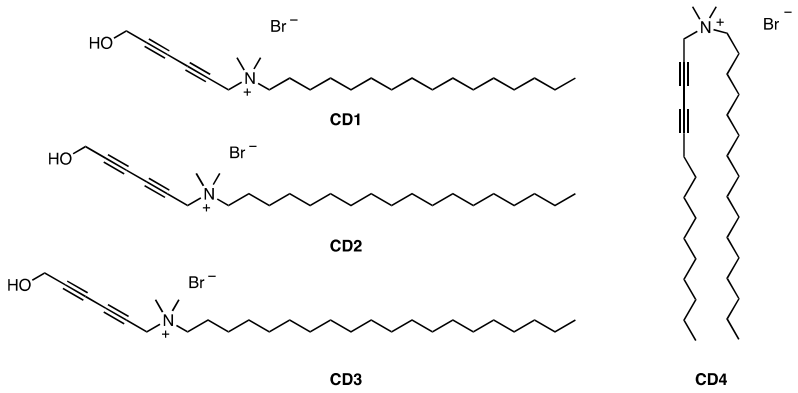

Chart 1. Molecular structures of the newly synthetized CDs **1-4**.

EXPERIMENTAL SECTION

Instrumentation. ^{1}H- and ^{13}C{^{1}H}-NMR spectra were recorded on a Bruker Avance II 300 spectrometer (operating at 300 for ^{1}H and 75 MHz for ^{13}C) or on a Bruker Avance 600 spectrometer (operating at 600.13 MHz for ^{1}H and 150.62 MHz for ^{13}C). Chemical shifts are

reported in δ values relative to tetramethylsilane, with reference to the solvent as internal standard for ^{1}H-NMR ($CDCl_3$ at 7.26 ppm; CD_3OD at 3.34 ppm) and for ^{13}C ($CDCl_3$ at 77.0 ppm; CD_3OD at 49.9 ppm), with coupling constants (J) given in Hz. HRMS-ESI spectra were recorded on a LTQ Orbitrap XL instrument. UV-vis measurements were carried out on Perkin Elmer Lambda 18 double beam spectrophotometer, absorbance normalized for optical path length and concentration was reported. Conductivity measurements were carried out on a HI-9932 Hanna conductivity meter equipped with a thermostat apparatus, in the temperature range 4–60 °C. All measurements were carried out in a jacketed cell maintained at the appropriate temperature (± 0.1 °C). Ultrasonic processor UP100H, ultrasonic power 100 Watts, titanium sonotrode MS 0.5 (tip diameter 7 mm), frequency 30 kHz, automatic frequency tuning system, amplitude adjustable 20-100%, pulse 0-100% was used for liposomes preparation. DLS measurements were performed with a Malvern Nano-ZetaSizer, equipped with a 5 mW HeNe laser (wavelength = 632.8 nm) and a digital logarithmic correlator. The normalized intensity autocorrelation functions were measured at an angle of 173° at 25.0 ± 0.1 °C. The autocorrelation functions were analyzed by using the cumulant fit. The first cumulant was used to obtain the apparent diffusion coefficients D of the particles, further converted into apparent hydrodynamic diameters, d_h, by using the Stokes–Einstein relationship $d_h=k_BT/3\pi\eta D$, where k_BT is the thermal

energy and η the solvent viscosity. The inverse Laplace transform (CONTIN) was also used to resolve correlation functions of multimodal system. Gel permeation chromatography (GPC) analyses were performed on a Hewlett Packard Series 1050 HPLC system equipped with a 1047A RI detector and a TSK gel alpha-4000 GPC column (Tosoh, Japan), using DMF with LiBr 0.1% w/w as the mobile phase. The system was coupled to Clarity software version 6.2 (DataApex, Prague, The Czech Republic) for signal processing. Surface pressure (π) measurements were carried out by means of a Wilhelmy plate (39.24 mm of perimeter) technique using a Langmuir Minitrough, KSV Instruments Ltd., Helsinki in Teflon with 325 mm of length and 75 mm width and total area of 24 380 mm^2 enclosed in a plexiglass box to reduce surface contamination.

Materials. PBS (Aldrich, 0.01 M phosphate buffer 0.0027 M KCl, 0.137 M NaCl, pH 7.4), pyrene, LiBr, CTAB and all reagents employed for the synthesis of CDs **1-4** were purchased from Sigma-Aldrich. CDHB was prepared according to a reported procedure.[31] The synthesis of compound **6** was performed according to the method reported in the literature.[32] CH_2Cl_2 was dried by distillation over P_2O_5 under nitrogen.

*6-Bromohexa-2,4-diyn-1-ol (**5**).* 1.0 g (9 mmol) of hexa-2,4-diyne-1,6-diol and 3.0 g (9 mmol) of CBr_4 were suspended in 15 mL of dry CH_2Cl_2 under nitrogen. The mixture was cooled to 0 °C and a solution of 2.5 g (9 mmol) of PPh_3 in 15 mL of anhydrous CH_2Cl_2 were added

drop-wise. The reaction was quenched after two hours by addition of MeOH and the solvent was removed under reduced pressure. The oily residue was purified by chromatography on silica gel (eluent hexane/AcOEt=5/1) to afford 0.48 g (2.8 mmol) of **5** (yield 31%). ^{1}H-NMR ($CDCl_3$, 300 MHz): δ = 4.354 (s, 2H, C*H*$_2$OH); 3.951 (s, 2H, CH_2Br); 2.572 (s, 1H, OH) ppm. $^{13}C\{^{1}H\}$-NMR ($CDCl_3$, 75 MHz): δ = 80.10, 75.35, 71.83, 71.07, 52.85, 5.36 ppm.

*N-hexadecyl-N-(6-hydroxyhexa-2,4-diynyl)-N,N-dimethylammonium bromide (CD**1**).* 0.85 mL (2.5 mmol) of *N,N*-dimethyl-*N*-hexadecylamine and 0.44 g (2.5 mmol) of **5** were dissolved in 30 mL of acetone and the mixture was heated to reflux for one day. The reaction was allowed to cool to room temperature obtaining 0.86 g (1.9 mmol) of crystallized product **1** (yield 76%) that resulted pure by elemental analysis. ^{1}H-NMR (CD_3OD, 300 MHz): δ = 4.501 (s, 2H, $NCH_2C\equiv C$), 4.298 (s, 2H, C*H*$_2$OH), 3.385-3.456 (m, 2H, CH_2CH_2N), 3.172 (s, 6H, $N(CH_3)_2$), 1.690-1.844 (m, 1H, C*H*$_2$CH$_2$N), 1.252-1.423 (m, 26H, $CH_3(CH_2)_{13}CH_2CH_2N$); 0.901 (t, $^{3}J_{HH}$ = 6.2 Hz, 3H, C*H*$_3$CH$_2$) ppm. $^{13}C\{^{1}H\}$-NMR (CD_3OD, 75 MHz): δ = 82.40, 76.38, 67.76, 66.92, 65.81, 55.53, 51.24, 50.88, 33.04, 30.73, 30.72, 30.68, 30.49, 30.14, 27.27, 23.72, 23.61, 14.40 ppm. HRMS: calculated for $C_{24}H_{44}NO$ $[M-Br^-]^+$: 362.3423; found: 362.3979.

*3-Bromopropargyl alcool (**6**).* 2.0 mL (39 mmol) of Br_2 were added to a solution of 8.0 g (0.143 mol) of KOH in 65 mL of water. After

cooling to 0 °C, 2.0 mL (35 mmol) of propargyl alcohol were added and the mixture was stirred at 0 °C for 3 h in the dark. Then the reaction mixture was extracted three times with diethyl ether and the combined organic layers were dried over Na_2SO_4, filtered and concentrated under reduced pressure to afford 3.9 g (29 mmol) of **6** (yield 83%). ^{1}H-NMR (CD_3OD, 300 MHz): δ = 2.475 (s, 1H, OH) 4.282 (s, 2H, CH_2) ppm. $^{13}C\{^1H\}$-NMR ($CDCl_3$, 75 MHz): δ = 78.21, 51.84, 45.83 ppm.

*6-(Dimethylamino)hexa-2,4-diyn-1-ol (**7**).* 14 mg (0.14 mmol) of CuCl were added to 6.5 mL of a 30 % *n*-$BuNH_2$ aqueous solution previously deoxygenated under Argon flush. After the blue mixture turned yellow by adding a few amount (tip of a spatula) of hydroxylamine hydrochloride, 0.91 mL (8.4 mmol) of *N*,*N*-dimethylpropargyl amine were added to the mixture. The mixture was cooled to 0 °C and 1.0 g (7 mmol) of **6** was added at once. More crystals of hydroxylamine hydrochloride were added throughout the course of reaction, as necessary, to prevent the solution from turning blue. After the reaction completion, the mixture was extracted three times with diethyl ether and the combined organic layers were dried over Na_2SO_4, filtered and concentrated under reduced pressure. The crude product was purified by chromatography on silica gel (eluent from CH_2Cl_2 to CH_2Cl_2/AcOEt = 4/1) to afford 0.71 g (5.1 mmol) of **7** (yield 74%). ^{1}H-NMR ($CDCl_3$, 300 MHz): δ = 4.331 (s, 2H, C*H*$_2$OH), 3.412 (s, 2H, CH_2N), 2.444 (s, 1H, OH), 2.357

(s, 6H, NMe_2) ppm. $^{13}C\{^1H\}$-NMR ($CDCl_3$, 75 MHz): δ = 75.91, 74.93, 69.90, 69.88, 51.37, 48.22, 43.86 ppm.

*CD **2** and **3**.* 0.50 g (3.6 mmol) of **7** and 1 equiv of alkyl bromide (either octadecyl for CD**2** or icosyl for CD**3**) were dissolved in 35 mL of acetone and the mixture was heated to reflux for one week. The reaction was cooled to room temperature and the residue obtained by removal of the solvent under reduced pressure was purified by crystallization in acetone/Et_2O providing 0.89 g (1.9 mmol) and 0.77 g (1.5 mmol) of amphiphiles **2** (yield 53%) and **3** (yield 43%), respectively.

*N-(6-hydroxyhexa-2,4-diynyl)-N,N-dimethyl-N-octadecylammonium bromide (CD **2**).* ^1H-NMR (CD_3OD, 300 MHz): δ = 4.534 (s, 2H, $NCH_2C\equiv C$), 4.321 (s, 2H, CH_2OH), 3.419-3.496 (m, 2H, CH_2CH_2N), 3.211 (s, 6H, NMe_2), 1.755-1.863 (m, 2H, CH_2CH_2N), 1.257-1.422 (m, 30H, $CH_3(CH_2)_{15}CH_2CH_2N$), 0.933 (t, $^3J_{HH}$ = 6.2 Hz, 3H, CH_3CH_2) ppm. $^{13}C\{^1H\}$-NMR (CD_3OD, 75 MHz): δ = 82.70, 76.61, 67.85, 66.94, 66.06, 54.63, 51.42, 50.90, 33.01, 30.75, 30.67, 30.65, 30.51, 30.44, 30.37, 30.01, 27.32, 23.77, 23.68, 14.36 ppm. HRMS: calculated for $C_{26}H_{48}NO$ $[M-Br^-]^+$: 390.3736; found: 390.4272.

*N-icosyl-N-(6-hydroxyhexa-2,4-diynyl)-N,N-dimethylammonium bromide (CD **3**).* ^1H-NMR (CD_3OD, 300 MHz): δ = 4.491 (s, 2H, $NCH_2C\equiv C$), 4.302 (s, 2H, CH_2OH), 3.394-3.463 (m, 2H, CH_2CH_2N), 3.187 (s, 6H, NMe_2), 1.758-1.863 (m, 2H, CH_2CH_2N), 1.255-1.424 (m, 34H,

$CH_3(CH_2)_{17}CH_2CH_2N$), 0.931 (t, $^3J_{HH}$ = 6.2 Hz, 3H, CH_3CH_2) ppm. $^{13}C\{^1H\}$-NMR (CD_3OD, 75 MHz): δ = 82.52, 76.51, 67.82, 67.03, 65.99, 55.75, 51.44, 50.90, 33.01, 30.70, 30.65, 30.54, 30.40, 30.36, 30.00, 27.21, 23.66, 14.31 ppm. HRMS: calculated for $C_{28}H_{52}NO$ $[M-Br^-]^+$: 418.4049; found: 418.4695.

*Pentadeca-2,4-diyn-1-ol (**8**).* Compound **8** (0.60 g, yield 37%) was prepared from compound **6** (1.00 g, 7.4 mmol) according to the procedure described above for the preparation of compound **7**. ^1H NMR ($CDCl_3$, 300 MHz, 298 K): δ = 4.321 (s, 2H, CH_2OH), 2.282 (t, *J* = 6.8 Hz, 2H, $-CH_2C\equiv C$), 1.604 (s, 1H, OH), 1.513 (qt, *J* = 6.8 Hz, 2H, $CH_2CH_2C\equiv C$), 1.196–1.458 (m, 14H, $-(CH_2)_7-$), 0.881 (t, *J* = 7.5 Hz, 3H, CH_3) ppm. $^{13}C\{^1H\}$-NMR ($CDCl_3$, 75 MHz, 298 K): δ = 82.02, 73.43, 71.05, 64.33, 51.68, 31.94, 29.52, 29.51, 29.38, 29.12, 28.84, 28.13, 22.72, 19.32, 14.11 ppm.

*N-hexadecyl-N,N-dimethyl-N-(pentadeca-2,4-diynyl)-ammonium bromide (CD**4**).* Compound **8** (0.46 g, 2.1 mmol) was dissolved in dry CH_2Cl_2 (15 mL) under nitrogen. The mixture was cooled to 0 °C, and a solution of PBr_3 (0.20 mL, 2.13 mmol) in CH_2Cl_2 (3 mL) was added dropwise. After two hours, the solvent was removed under reduced pressure and the oily residue was purified by chromatography on silica gel (eluent: $CHCl_3$) to afford the desired product (0.52 g, 1.8 mmol, yield 89%) that was dissolved in acetone (5 mL) with *N,N*-dimethylhexadecylamine (0.68 mL, 2.0 mmol). The mixture was

heated to reflux for one day. After cooling to room temperature, the precipitate was isolated and crystallized from Et_2O to afford amphiphile CD **4** (0.38 g, yield 60%) that resulted pure by elemental analysis. ^{1}H NMR ($CDCl_3$, 300 MHz, 298 K): δ = 4.901 (s, 2H, $-CH_2N$), 3.594 (m, 2H, CH_2CH_2N), 3.463 (s, 6H, NMe_2), 2.291 (t, J = 7.4 Hz, 2H, $-CH_2C{\equiv}C$), 1.734 (s, 2H, $-CH_2CH_2N$), 1.546 (qt, J = 7.4 Hz, 2H, $-CH_2CH_2C{\equiv}C$), 1.192–1.413 (m, 40H, $CH_3(CH_2)_7CH_2CH_2C{\equiv}C$, $CH_3(CH_2)_{13}CH_2CH_2N$), 0.864 (t, J = 6.5 Hz, 6H, $-CH_2CH_3$) ppm. $^{13}C\{^1H\}$-NMR ($CDCl_3$, 75 MHz, 298 K): δ = 84.61, 64.24, 63.53, 62.38, 55.46, 50.65, 31.91, 31.87, 29.72, 29.61, 28.96, 27.9, 26.2, 22.94, 22.73, 19.31, 14.10 ppm. HRMS: calculated for $C_{33}H_{62}N$ $[M-Br]^+$: 472.4923; found: 472.5401.

Methods

*Determination of Krafft point (T_K) and Krafft temperature of **CDs 1-3**.* T_K values of CDs **1-3** were determined by measuring the temperature-scan conductivity on 20 mL sample of 20 mM surfactant solutions in the temperature range 10-60 °C according to a described procedure.[33] During the measurements, the solution was continuously stirred and the temperature was raised at a rate of 0.2 °C/min. The error in the conductivity measurements was within ± 0.1%. The T_k was defined as the temperature at which conductivity begins to rise abruptly, whereas the Krafft temperature relative

to the chosen concentration is the temperature above which the specific conductivity remains constant.

*Determination of critical micellar concentration (cmc) of CD **1-3.*** Known volumes of stock solutions of CD **1-3** were added at 60 °C to 30 mL of deionized water to carry out conductivity measurements after mixing and temperature equilibration. The *cmc* value for each amphiphile is determined by the intercept point of the two linear trends obtained by plotting the specific conductivity versus the concentration of amphiphile.

*Determination of the critical aggregation concentration (cac) of CD **4** by fluorescence measurements.* The *cac* of CD **4** was measured at 25 °C by a reported procedure that exploits the variation in the intensity of the vibronic fine structure of pyrene monomer emission spectrum upon association with aggregates.[34] Aqueous solutions (3 mL) of CD **4** between 10 μM and 80 μM were added to a defined amount of pyrene in order to obtain a final concentration of ~0.5 μM (prepared from 7 μL of a 160 μM stock solution of pyrene in absolute ethanol degassed under a nitrogen flux). The solutions were kept at 40 °C, under stirring, for 12 h. Emission spectra of the solutions were acquired in the range 350–450 nm (λ_{exc} = 335 nm). The *cac* was defined as the concentration where the plot of intensity ratio of the third (I_3, 380 nm) and first (I_1, 370 nm) vibronic peaks of pyrene I_3/I_1 *versus* CD **4** concentration begins to rise.

*Preparation of CD **4** liposomes.* Liposomes formed by CD **4** were prepared according to the method of injection/sonication.[35] Briefly, a proper amount of CD **4** was dissolved in dimethylsulfoxide and injected into an opportune volume of water under heating at 80 °C and vigorous stirring to give a 5mM liposomal suspension. Liposome suspension was exposed to acoustic energy from a tip probe sonicator in order to reduce the multilamellarity of the vesicles

and homogenize their dimensions. The exposure time to sonication (15 minutes, 70 Watts, pulsed-power mode) determines the size of the vesicles.[36] Lastly, before polymerization liposomes were stored at 4 °C for at least 6 h to obtain crystallization of lipid membranes.

Determination of aggregates size by DLS. Measurements were performed on micellar samples containing sodium bromide as added electrolyte to minimize the effects of counterion cloud fluctuations on the dynamic of ionic micelles in solution.[37-38] The concentration of added electrolyte was observed to affect the size of the aggregates and is was adjusted depending on the surfactant type and concentration to optimize the scattered light intensity. Temperature scans revealed a decreasing trend of the aggregate size of CD1-3 by heating, as observed for several ionic surfactants self-assembling in wormlike micelles.[39] The data at the highest accessible temperature (60 °C), far from the Krafft point were reported for these samples. DLS measurements were carried out on aqueous micellar solutions of CD **1** [75 mM] at 60 °C in NaBr 100 mM, CD **2** [25 mM] at 60 °C in NaBr 50 mM, CD **3** [5 mM] at 60 °C in NaBr 15 mM and on CD **4** liposomes. All aggregates were analyzed by DLS measurements soon after preparation, and after irradiation. Measurements were repeated after 48 h.

Irradiation of CDs in aggregative conditions. Micellar solutions of amphiphiles **1-3** at 60 °C were irradiated at 254 nm for 2 h by using a low-pressure mercury UV-lamp (Spectroline EF-140C).

Polymerization was carried out on a) aqueous solutions of 0.06 mM CD **1(2, 3),** b) aqueous solutions of 76 mM CD **1(2, 3)** and 150 mM NaBr and c) deuterated aqueous solutions of 76 mM CD **1(2, 3)** and 150 mM NaBr.

GPC elution. Samples for GPC analysis were prepared dissolving either the monomer or polymerized CD **1** in DMF with 0.1% LiBr w/w (final concentration of ~1 mg/mL). The polymerized CD **1** sample was obtained by i) irradiating at 254 nm 10 mL of 0.06 mM aqueous solution for 2 h at 60 °C, ii) removing the water under high vacuum.

Langmuir trough measurements. CD **1(3-4),** CTAB and CDHB monolayers were prepared using PBS as subphase. The minitrough was thermostated in a 25 °C bath. A volume of 10 µL of lipid solution (1.0 mg/mL dissolved in $CHCl_3$) was spread over the aqueous subphase using a Hamilton microsyringe. After the deposition, the solvent was allowed to evaporate for 5 minutes at an initial pressure lower then 1 mN/m before starting three cycles of compression/expansion up to π = 3 mN/m to stabilize lipid monolayer by moving the nylon barriers at a constant rate of 50 mm/min. The isotherms were registered closing completely the barriers (target to stop at π = 100 N/m). Different isotherms on independent samples were carried out several times to verify their reproducibility. The reported isotherms are the average of at least three different and

independent runs. The experimental error for the final concentration of each sample was estimated by means of the error propagation, being in the order of ± 2.5 % for the reported values. For calculation, we considered the error of the analytical balance to be ± $0.5 \cdot 10^{-4}$ g, and the error of Hamilton syringe of ±1.25 % of nominal volume.

RESULTS AND DISCUSSION

*Synthesis and characterization of CDs **1-4**.* CDs **1-4** are characterized by a novel molecular structure where the polymerizable diacetylenic moiety is located close to the ammonium headgroup. To prepare CD **1** (Scheme 2), the commercially available hexa-2,4-diyne-1,6-diol was mono-brominated according to a reported procedure carried out in Apple's conditions[40] and the resulting product was used for the alkylation of the *N,N*-dimethylhexadecylamine. The latter reaction was carried out at reflux in acetone, which was found to be a good solvent for the subsequent crystallization of CD **1**.

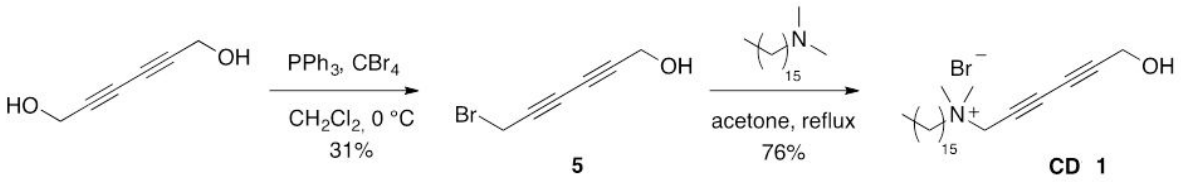

Scheme 2. Synthetic pathway to obtain amphiphile CD **1**

For the preparation of CDs **2**-**3** (Scheme 3), a different procedure was followed because *N*,*N*-dimethyloctadecyl- and *N*,*N*-dimethylicosylamine are not commercially available. Therefore the diacetylenic moiety was obtained through Cadiot-Chodkiewicz coupling between 3-bromopropargyl alcohol **6**, obtained by a reported procedure,[32] and commercially available *N*,*N*-dimethylpropargyl amine. Coupling adduct **7** was then alkylated with octadecyl- or icosylbromide, in the same conditions used for obtaining CD **1**, to afford CD **2** and CD **3**, respectively. However, in these cases, the quaternization reaction required much longer time probably because of the lower electrophilicity of the used alkylbromides with respect to that of compound **5** involved in the preparation of CD **1**.

Bromo-alkyne **6** was also involved in the preparation of amphiphile CD **4** through Cadiot-Chodkiewicz coupling with 1-dodecyne to afford alcohol **8** that was successively brominated with PBr_3 and used as alkylating agent of *N*,*N*-dimethylhexadecylamine to obtain CD **4**.

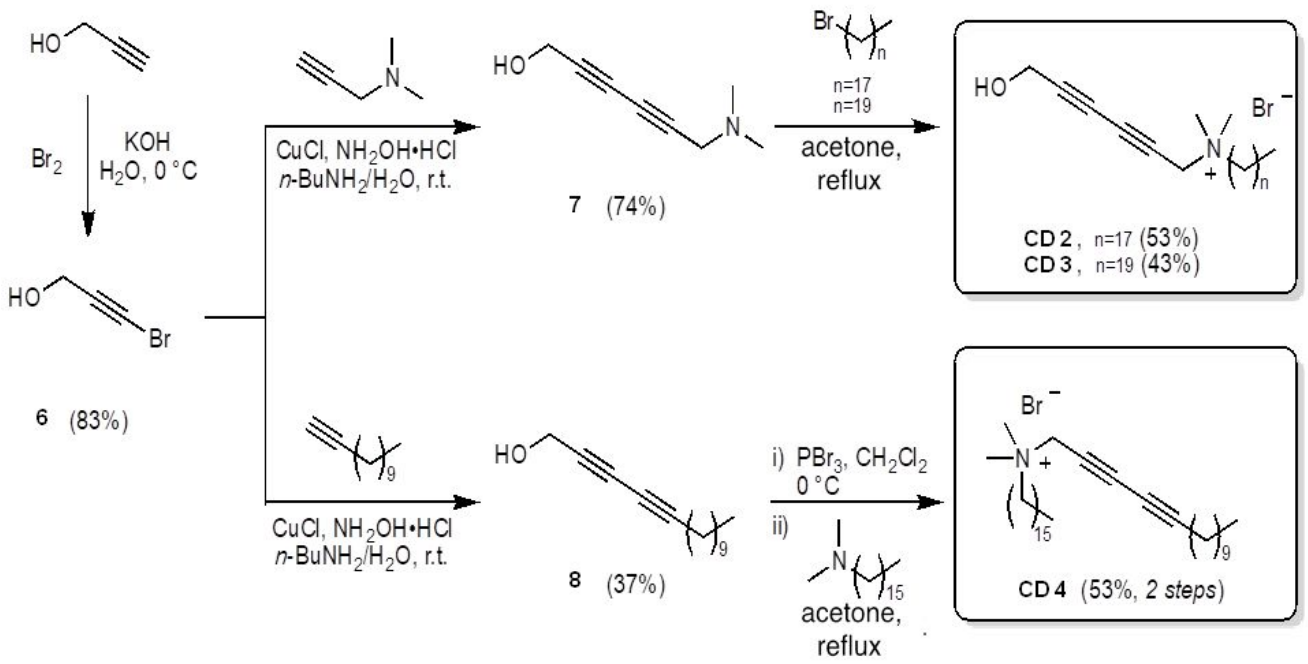

Scheme 3. Synthetic pathways to obtain amphiphiles CDs **2–4**

In order to define the temperature/concentration domain in which CDs **1-3** form aggregates, Krafft point-temperature T_K and *cmc* (at $T > T_K$) of amphiphiles were measured by conductivity experiments. As expected, the value of T_K and that of *cmc* increases and decreases, respectively, as the hydrophobic chain becomes longer (Table 1).

Table 1. Physicochemical features of CDs

CD	T_K / °C[a]	*cmc/cac* [a] [M]	D_h (nm)[b]	PDI[b]
1	27	$(8.0 \pm 0.4)\cdot10^{-6}$ [60 °C]	8 [60 °C]	0.24
2	35	$(5.5 \pm 0.3)\cdot10^{-6}$ [60 °C]	20 [60 °C]	0.48
3	42	$(1.0 \pm 0.3)\cdot10^{-6}$ [60 °C]	33 [60 °C]	0.22
4	<4	$(7.0 \pm 0.5)\cdot10^{-6}$ [25 °C]	310[d] [25 °C]	0.21

[a]1-4 Krafft point (T_K) and *cmc*/*cac* were determined in deionized water; [b]experimental conditions of DLS measurements: 75 mM CD **1** at 60 °C in 100 mM NaBr; 25 mM CD **2** at 60 °C in 50 mM NaBr; 5 mM CD **3** at 60 °C in 15 mM NaBr; 5 mM CD **4** at 25 °C in H_2O; hydrodynamic diameters D_h and polydispersity indexes (PDI) were obtained from cumulant analysis, typical CONTIN distributions for some samples are reported in the supplementary information. T_K were determined with an accuracy of ± 0.1 °C; error in determination of D_h is within ± 5% of the value. [d]Reported data refer to CD**4** liposomes.

DLS analyses of CD solutions above *cmc* and T_K reported in Table 1 indicated the presence of aggregates consistent with spherical or worm-like shaped micelles in the case of CDs **1-3** (D_h values of 8, 20 and 33 nm, respectively) and with vesicular aggregates in the case of CD **4** (D_h ~ 300 nm). In the case of CD **4**, the value at which lipids begin to self-assembly into bilayers, properly named critical aggregative concentration (*cac*), was assessed by a method that exploits pyrene as fluorescent probe.[34]

Irradiation of CDs and assessment of polymerization by UV-vis measurements. The photopolymerization of CDs in aggregating conditions (micellar and vesicular aggregates formed by CDs **1-3** and CD **4**, respectively) was investigated.

Extended diacetylene polymerization is known to yield colored samples due to extended π-conjugated *ene-yne* backbone with absorption at high frequencies.[4] However, in the case of micellar

aggregates, diacetylene polymerization was not expected to yield a colored solution, because the low aggregation number of micelles would limit the extent of the conjugated backbone.[41] Therefore, in the case of micellar aggregates, the occurrence of polymerization is generally assessed by the appearance of new bands in the UV spectrum. Concentration was expected to play a major role in the occurrence of polymerization by controlling the state of phase of aggregates and hence the relative topology of diacetylene residues within the micelle. Micelle solutions of amphiphiles CDs **1-3** at different concentrations - ranging from 0.06 to 60 mM - were irradiated for two hours at 60 °C (*i.e.* above the T_K of amphiphiles). Surprisingly the evidence of PDA formation was observed, for all amphiphiles, in the case of 0.06 and 0.6 mM samples, whereas polymerization occurred at a lower or negligible extent for more concentrated solutions (Figure 1).

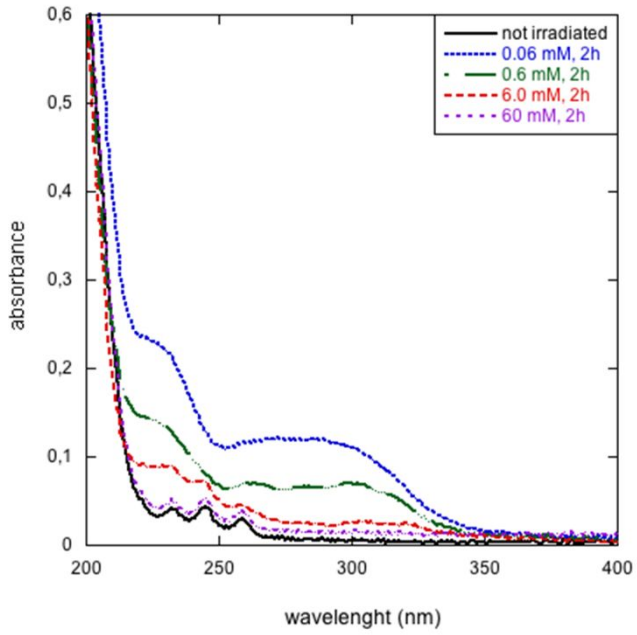

Figure 1. Absorption spectra of aqueous CD **1** solutions recorded after two hours of irradiation carried out at 60 °C and different concentrations: 0.06 (blue dotted trace), 0.6 (green dashed dotted trace), 6.0 (red dashed trace) and 60 (purple dashed trace) mM; black solid trace is referred to the non-irradiated sample 0.06 mM. An analogue behavior was observed in the case of CD **2** and CD **3**.

Actually, in agreement with literature reports on PDA micelles,[41, 42] two broad bands appeared in the region between 220 and 350 nm of the absorption spectra upon irradiation of 0.06 and 0.6 mM samples, the highest values of absorbance being observed in the case of 0.06 mM sample. Polymerization of 0.06 mM samples was investigated by recording the UV spectra over time during irradiation. A net change of the UV spectra was detectable yet after 15 minutes of irradiation for all three amphiphiles. The highest extent of polymerization occurred within one hour (Figure 2), then polymerization rate decreased and no significant changes were detected in the next hour (Figure 2d). Absorption maxima were observed at slightly different wavelengths in the case of the three amphiphiles: ~280 nm for CD **1**, and ~302 nm for both CD **2** and CD **3** (Figure 2a-2c). This result could indicate a more extended conjugation in the case of CDs **2-3** with respect to CD **1**. Further,

in the case of CD **3**, the maximum of absorbance of the PDA-associated band was the most intense (*i.e.* 0.17); this result could be related to the lowest value of *cmc*.

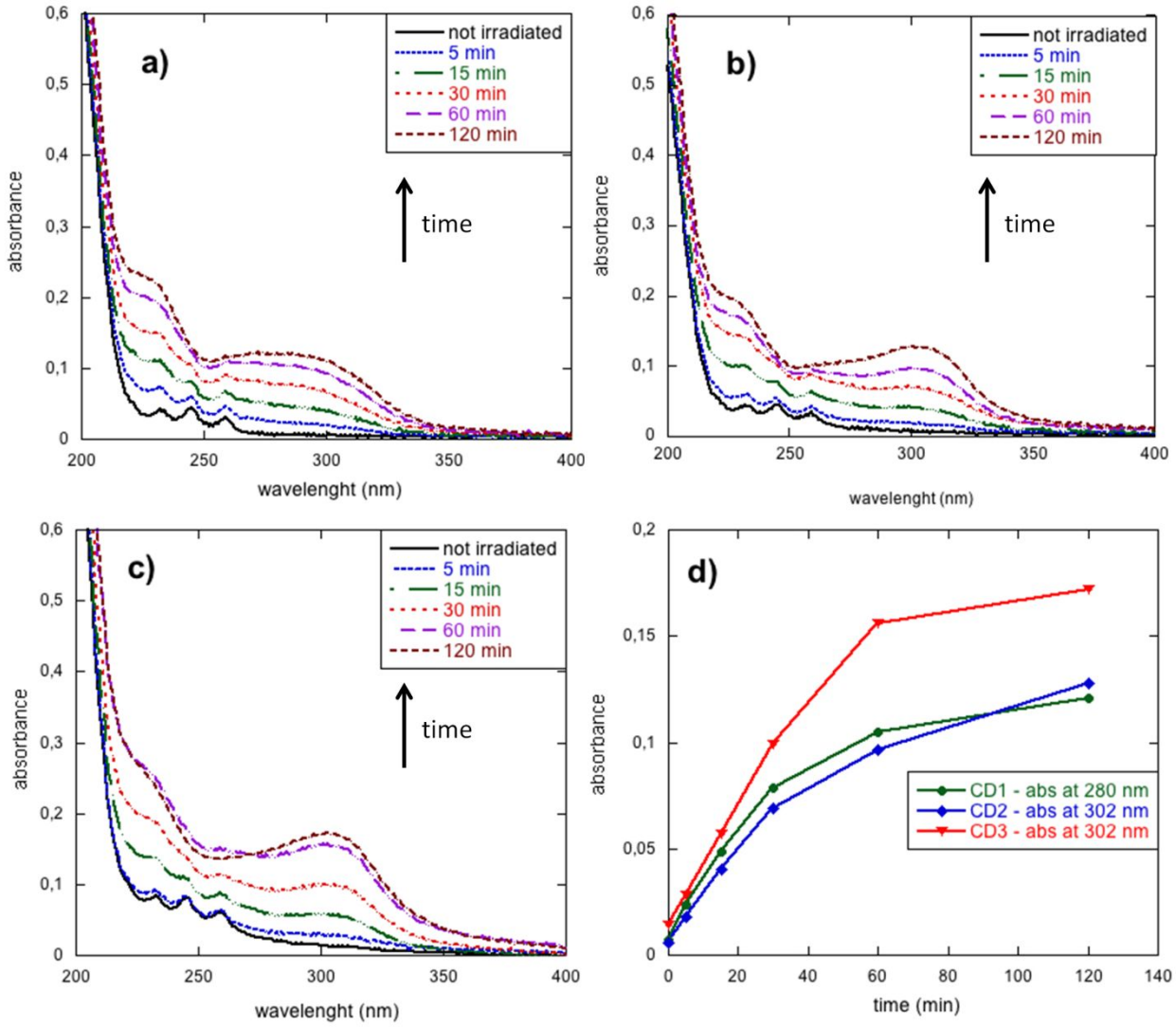

Figure 2. Absorption spectra of 0.06 mM aqueous solutions of a) CD**1**, b) CD**2** and c) CD**3** recorded at fixed times of irradiation at 60 °C; d) evolution of intensity of absorption maximum as a function of irradiation time.

A further evidence of the occurrence of polymerization was provided by GPC performed on monomeric and polymerized samples of CD **1**. In fact, the chromatogram relative to the non-irradiated sample displayed a sharp peak (retention time ~16 min) of the monomer whereas that relative to the irradiated sample showed a slightly broad peak at lower retention time (*i.e.* ~14 min) attributable to the polymer (Figure 3).

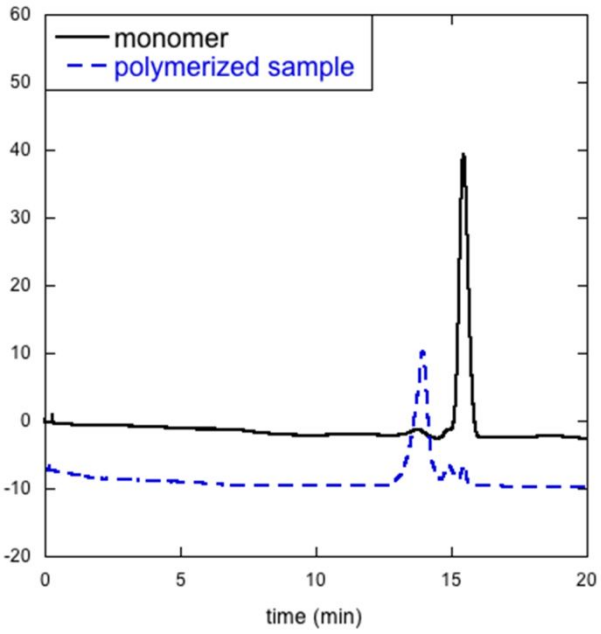

Figure 3. GPC chromatograms relative to monomeric (black solid trace) and polymerized (blue dashed trace) samples of CD **1** (eluent DMF with LiBr 0.1% w/w).

Polymerization upon UV irradiation of CD **4** vesicular aggregates prepared according to the method of injection/sonication was investigated in different aqueous media, *i.e.* water, PBS 150 mM and PBS 15 mM. DLS analysis before and after irradiation indicated

the presence of a stable monomodal distribution of vesicles featuring a hydrodynamic diameter of ~300 nm in both water and PBS buffers. In all polymerization experiments, both the lack of color detectable with naked eye and the absence of typical bands in the UV spectrum indicated that polymerization did not occur. The failure of polymerization of CD **4** liposomes as well as that of CDs **1-3** aggregates at high concentration should be due to an unfavorable arrangement of diacetylene moieties.

*Investigation on CD **1** arrangement in aggregating conditions.*

The extension of solid-state reactivity conditions to colloidal systems suggests that polymerization of the diacetylenic function into an *ene-yne* polymer requires a specific topology/alignment of the diacetylenic moieties. Therefore, further investigations were carried out to assess the topology of the diacetylenic functions of amphiphile CDs **1-3** within their micellar aggregates, aimed at understanding the results of polymerization experiments. In fact, the hydrophobic diacetylenic function could be folded in the hydrophobic region of the micelle or, due to the presence of the terminal hydroxyl group, lay at the water/micelle interface, perpendicular to the hydrophobic chains, thus being exposed to water. ROESY NMR experiments aimed at elucidating this point were carried out on 0.06 and 60 mM (*i.e.* in proximity of and largely above the *cmc*, respectively) aqueous solutions of CD **1** chosen as

testing molecule at 45 °C (*i.e.* above the T_K). Further, a long range ^1H-^{13}C heteronuclear correlation experiment (HMBC) was carried out to univocally assign the signals of methylenic protons adjacent to diacetylenic function. In fact, such protons give similar NMR signals in terms of multiplicity and chemical shift in ^1H NMR spectrum (*i.e.* singlets at 4.46 and 4.69 ppm in D_2O). The HMBC spectrum allowed to attribute the signal at 4.69 ppm to the propargylic protons next to the charged nitrogen by means of three-bond coupling with the carbons adjacent to the quaternary nitrogen, *i.e.* those of the two methyl groups and the first methylene of the hexadecyl chain.

ROESY spectrum of 60 mM aqueous solution of CD **1** shows a correlation peak between the signal due to the methylene adjacent to the hydroxyl group and those due to methylene groups of the hexadecyl chain, thus indicating that the hydroxyhexadiynyl substituent is folded toward the hydrophobic region of the micelle (Figure 4).

In the case of 0.06 mM sample, the absence of an analogous correlation peak did not provide a definite indication, because it could be ascribed to the occurrence of loose aggregates where the distance between lipid components does not allow a NOE effect.

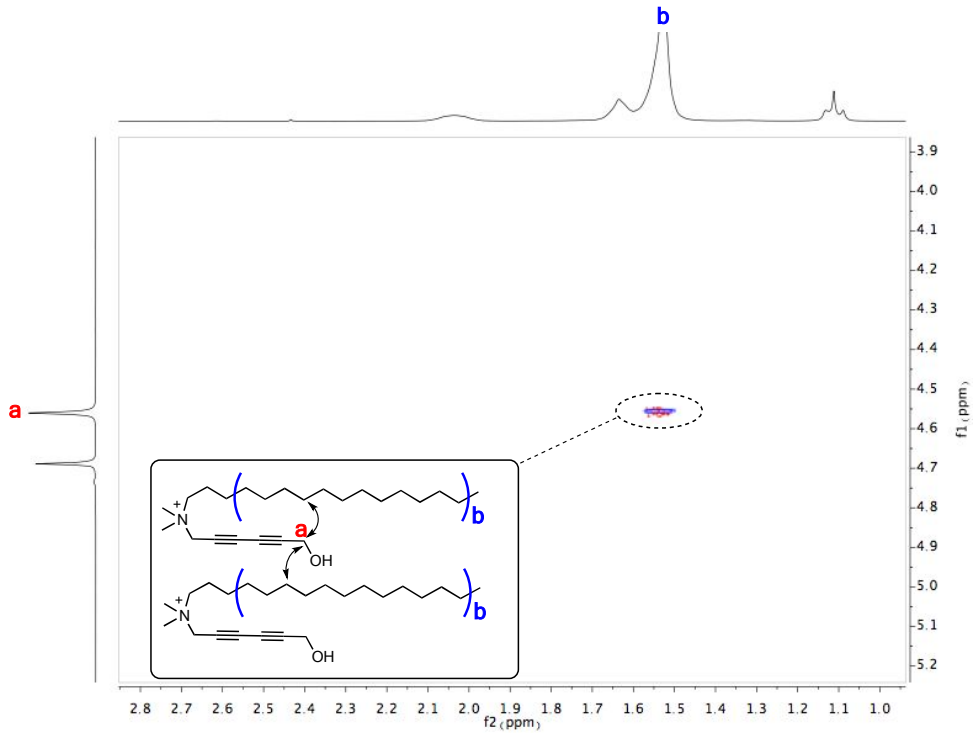

Figure 4. Region of ROESY spectrum of the 60 mM sample of CD1 in D_2O and representation of the topology of amphiphiles within the aggregates; folding of hydroxyhexadiynyl group in the hydrophobic region of the micelle is consistent with the presence of the correlation peak between the methylene group adjacent to the hydroxyl group (4.46 ppm) and those of the hexadecyl chain.

Langmuir trough experiments. To support the hypothesis of the folding of the hydroxyhexadiynyl chain suggested by the results of the ROESY experiment, we carried out Langmuir trough experiments to obtain Langmuir compression isotherms of CD **1**, CTAB and CDHB. Non-polymerizable CTAB and CDHB were chosen because the only difference between each of them and CD **1** concerns a substituent on the ammonium nitrogen, namely hydroxyhexadiynyl (CD **1**), methyl

(CTAB) and hydroxyethyl (CDHB), and the differences in their π/A compression isotherms can be directly related to their different substituents; therefore they can be good comparison systems to investigate the topology of the hydroxyhexadiynyl residue in the lipid film. In fact, in the lipid monolayer at the air water interface the hydroxyethyl residue of CDHB should be exposed to the water phase thus giving a compression isotherm similar to CTAB. If the hydroxyhexadiynyl residue of CD **1** were exposed to water the compression isotherm of its monolayer should be analogous to those of CTAB and CDHB. The obtained π/mean molecular area (A_h) isotherms are reported in Figure 5A.

The obtained monolayers were stable and in equilibrium conditions, as proven by the fact that the isotherms obtained by the compression/expansion cycles process were pretty similar to those obtained by closing completely the barriers.

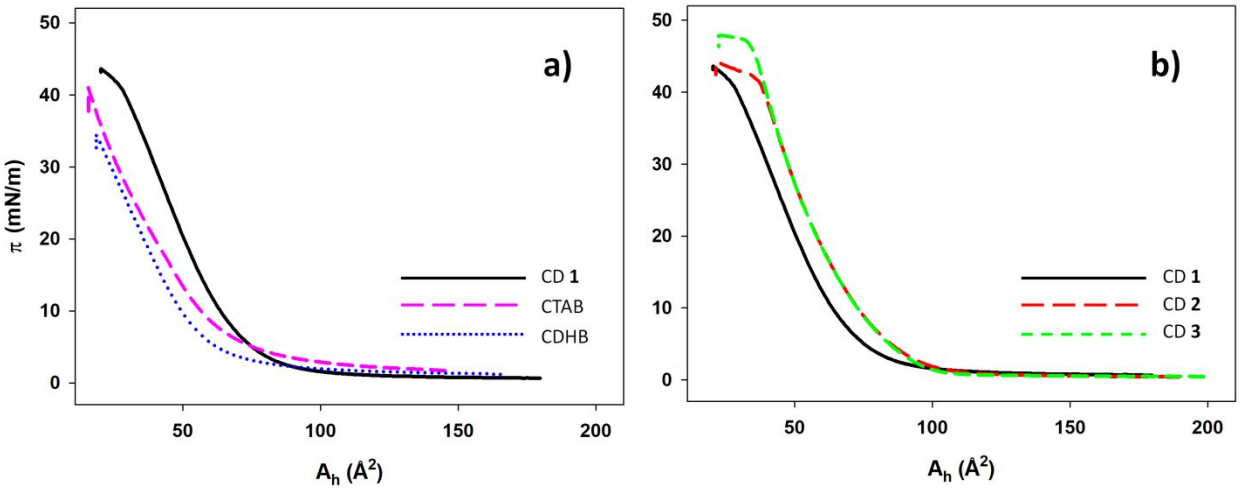

Figure 5. π–A isotherms of monolayers of CD **1** (black line in A and B) and A) CTAB (purple line), CDHB (blue line); B) CD **2** (red line) and CD **3** (green line) monolayers.

It can be clearly observed that all the isotherms of CD **1**, CTAB and CDHB show a similar behavior (Figure 5A), undergoing the transition from the liquid-expanded (LE) phase to the liquid-condensed (LC) phase up to the closure of the barriers. However, in the isotherm of CD **1** π rises at higher A_h, in fact in correspondence of the same A_h the π of the isotherms of CTAB and CDHB monolayers is lower with respect to π of the isotherm of CD **1**. Furthermore, in the case of CD **1** it seems that the monolayer does not reach the collapse condition differently from the monolayers of CTAB and CDHB. This finding indicates that the extent of lipid packing in CD **1** monolayer is reduced with respect to CTAB and CDHB ones, thus suggesting that the diacetylenic segment does not protrude toward the subphase, as it happens for the methyl group of CTAB and the hydroxylethyl group of CDHB, but is rather folded toward the hydrophobic region (Figure 6), in agreement with what suggested by NMR experiments.

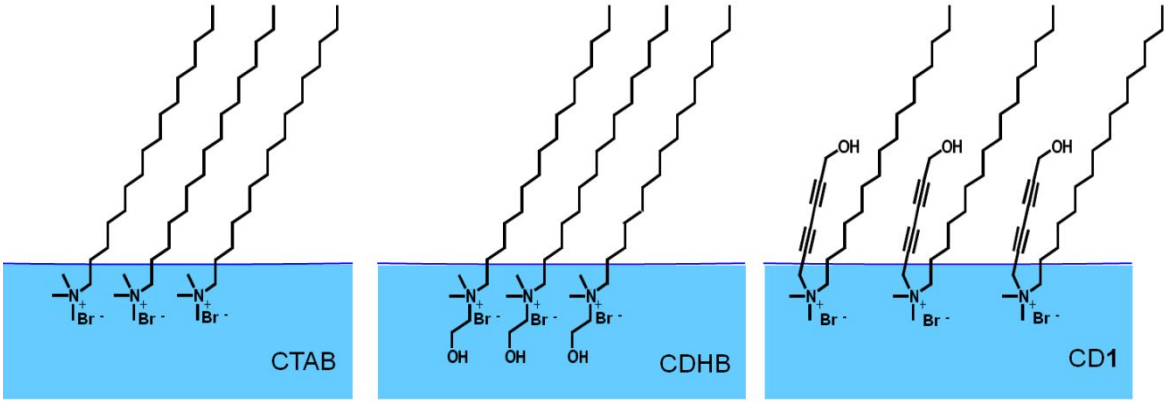

Figure 6. Schematic representation of CTAB and CDHB with the hydroxylethyl group protruding toward the subphase, and CD **1** monolayer with the diacetylenic segment folded toward the hydrophobic region.

To evaluate the effect of the chain length on the arrangement of diacetylenic functions and on the organization of the unimers in the aggregates we investigated also Langmuir monolayers of CDs **2** and **3** and compared their π-A compression isotherms with that of CD **1** (Figure 5B). The shape of the π/A_h curves is very similar, though in a homologous series a longer chain should correspond to a steeper isotherm,[43] and, in the case of CDs **2** and **3**, π begins to rise (*i.e.* the LC phase begins to form) at slightly larger A_h with respect to what observed with CD**1**. Further, in the isotherms of CDs **2** and **3** the plateau and the collapse are clearly observable (at 43 mN/m and 48 mN/m for **2** and **3**, respectively, indicating CD **3** monolayer as more stable), whereas in the case of CD **1** only the

beginning of a plateau (indicating that the lipid monolayer is close to the collapse) is observable. Moreover, in a homologous series, π should decrease as a function of increasing chain length for the transition from LE to the LC, whereas no difference was observed between CD **2** and CD **3** and the isotherm of CD **1** shows a different trend with slightly lower π with respect to the higher homologues. It is possible that the organization of the rigid diacetylenic function within the lipid bilayer contrasts at different extent the van der Waal's attraction between alkyl chains as observed in lipid monolayers formed by molecules with a rigid headgroup and alkyl chains of different length.[44, 45]

To obtain further information on the packing of the monolayer, the two-dimensional compressibility of each compression isotherm was investigated according to equation 1:

$$Cs^{-1} = -A_{\Pi} (d\pi/dA) \quad (1)$$

where Cs^{-1} is the compression modulus and A_{Π} is the area per molecule at the corresponding π. The plots of Cs^{-1} as a function of π reflect the fluidity/elasticity of the monolayers. The maximum in each curve corresponds to the state at which the monolayer features the minimum compressibility (*i.e.* the maximum packing of the lipid film) and the minimum fluidity.[46] The obtained Cs^{-1} are reported in Figure 7.

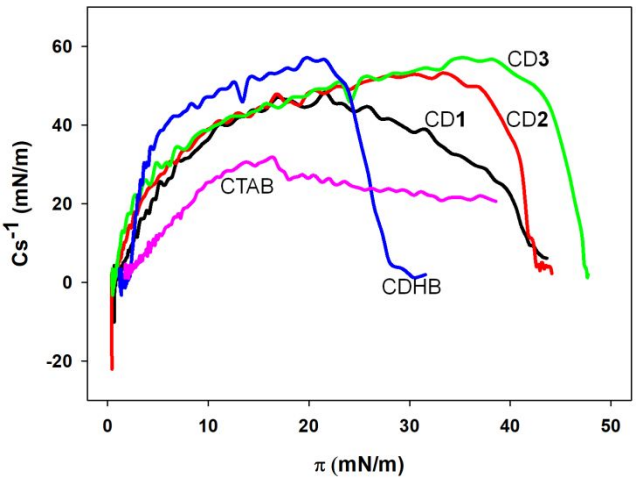

Figure 7. Compressibility modulus of CTAB (purple line), CDHB (blue line), CD**1** (black line), CD**2** (red line) and CD**3** (green line) monolayers.

It is clearly observable that CTAB monolayer features the highest compressibility whereas CDHB, CDs **2** and **3** are characterized by the lowest compressibility, even if at different π. The monolayer formed by CD **1** at π higher than 25 mN/m is the most compressible among those formed by investigated CDs. Moreover, the symmetry of the peak indicates that the transition from LE to LC phase consists of a single molecular reorientation, whereas the asymmetry of the peak relative to CD **2** and CD **3** denotes that two or more steps, *i.e.* different reorganization of the lipid molecules, occur during the transition.[46]

The results of our experiments and the knowledge of the typical phase-behavior of surfactant solutions allow some speculation on the observed polymerizability of CDs within their aggregates. At

concentrations largely above the *cmc*, CDs **1-3** probably yield highly compact aggregates in which the modest molecular mobility in proximity of water interface hampers the proper alignment of diacetylenic moieties in terms of γ angle. The failure of polymerization in the case of CD **4** liposomes can be ascribed to analogous reasons.

On the other hand, at concentrations close to the cmc, CDs **1-3** aggregates could exhibit a loose organization - consistent with the absence of intermolecular NOE effect - where the mobility of unimers can allow achieving the optimal arrangement of the diacetylene moieties for 1,4-addition (Scheme 4).

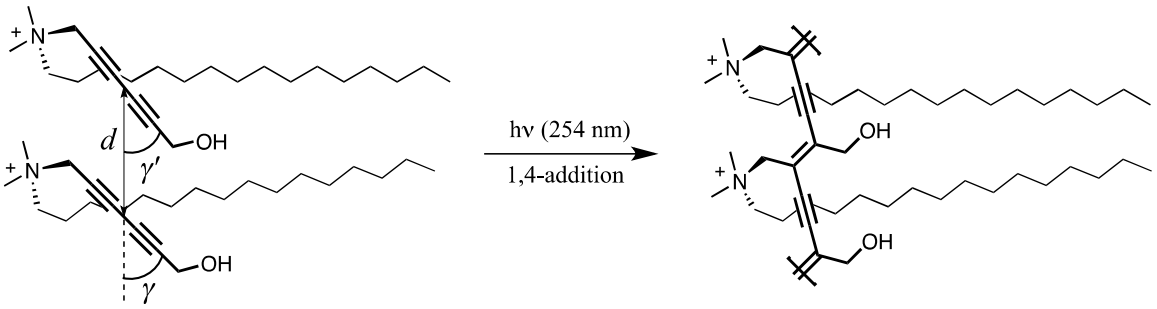

Scheme 4. Topology of diacetylenic residues for the polymerization of CD **1** within the aggregates. At concentrations not largely above the cmc, the loose structure of the aggregates could allow the appropriate alignment of diacetylene moieties for the occurrence of 1,4-addition. The folding of the hydroxyhexadiynyl toward the hydrophobic region of the micelle has been deduced from the ROESY and Langmuir through measurements.

CONCLUSIONS

Three structurally related micelle forming CDs **1-3** bearing two conjugated triple bonds in the headgroup were prepared and their aggregation and polymerization properties were investigated. The micelles polymerized upon irradiation by 1-4 addition of the diacetylene moieties, although colored aggregates were not formed. Also liposome forming twin CD **4**, where conjugated triple bonds are located in the hydrophobic tail in proximity of the headgroup, was synthesized and characterized. Our results pointed out that the ability to polymerize in aggregative conditions for these CDs strongly depend on their concentration in solution. Moreover, it seems that the length of the alkyl chain influences the rate and the extent of polymerization.

Polymerization of CD **1-3** in some aggregating conditions suggests that their inclusion in differently organized aggregates, such as liposomes, could favor optimal alignment of diacetylenic functions yielding more extended polymerization suitable for sensing applications.

AUTHOR INFORMATION

Corresponding Author

*giovanna.mancini@uniroma1.it

Author Contributions

The manuscript was written through contributions of all authors. All authors have given approval to the final version of the manuscript.

Acknowledgments

The authors acknowledge technical support by Mr. Enrico Rossi. GM and MB acknowledge financial support from a MIUR PRIN project entitled “BacHounds: Supramolecular nanostructures for bacteria detection”.

REFERENCES

(1) Banerjie, A.; Lando, J. B.; Yee, K. C.; Baughman, R. H. Characterization of the ladder polymerization of a crystalline cyclotetradiyne monomer. *J. Polym. Sci. Part B Polym. Phys. Ed.* **1974**, *12*, 1511.

(2) Lauher, J. W.; Fowler, F. W.; Goroff, N. S. Single-crystal-to-single-crystal topochemical polymerizations by design. *Acc. Chem. Res.* **2008**, *41 (9)* , 1215.

(3) Wegner, G. Polymerisation von derivaten des 2.4-hexadiin-1.6-diols in kristallinen Zustand. *Z. Naturforsch., Teil B* **1969**, *24 (7)* , 824.

(4) Yarimaga, O.; Jaworski, J.; Yoon, B.; Kim, J.-M. Polydiacetylenes: supramolecular smart materials with a structural hierarchy for sensing, imaging and display applications. *Chem. Commun*. **2012**, *48*, 2469.

(5) Seo, D.; Kim, J. Effect of the molecular size of analytes on polydiacetylene chromism. *Adv. Funct. Mater*. **2010**, *20*, 1397.

(6) Qian, X.; Städler, B. Recent developments in polydiacetylene-based sensors. *Chem. Mater.* **2019**, *31 (4)* , 1196.

(7) Charych, D. H.; Nagy, J. O.; Spevak, W.; Bednarski, M. D. Direct colorimetric detection of a receptor-ligand interaction by a polymerized bilayer assembly. *Science* **1993**, *261 (5121)*, 585.

(8) Ma, Z.; Li, J.; Liu, M.; Cao, J.; Zou, Z.; Tu, J.; Jiang, L. Colorimetric detection of *Escherichia coli* by polydiacetylene vesicles functionalized with glycolipid. *J. Am. Chem. Soc.* **1998**, *120,* 12678.

(9) Chen, X.; Kang, S.; Kim, M. J.; Kim, J.; Kim, Y. S.; Kim, H.; Chi, B.; Kim, S.-J.; Lee, J. Y.; Yoon, J. Thin-film formation of imidazolium-based conjugated polydiacetylenes and their application for sensing anionic surfactants. *Angew. Chem., Int. Ed*. **2010**, *49*, 1422.

(10) Chance, R. R.; Baughman, R. H.; Müller, H.; Eckhardt, C. J. Thermochromism in a polydiacetylene crystal. *J. Chem. Phys.* **1977**, *67*, 3616.

(11) Ahn, D. J.; Lee, S.; Kim, J.-M. Rational design of conjugated polymer supramolecules with tunable colorimetric responses. *Adv. Funct. Mater.* **2009**, *19*, 1483.

(12) Cheng, Q.; Stevens, R. C. Charge-induced chromatic transition of amino acid-derivatized polydiacetylene liposomes. *Langmuir* **1998**, *14 (8)* , 1974.

(13) Bloor, D. Dissolution and Spectroscopic Properties of the Polydiacetylene Poly(10,12-docosadiyne-1,12-diol-bisethylurethane). *Macromol. Chem. Phys.* **2001**, *202*, 1410.

(14) Berda, E. B.; Johan Foster, E.; Meije, E. W. Toward controlling folding in synthetic polymers: fabricating and characterizing supramolecular single-chain nanoparticles. *Macromolecules* **2010**, *43 (3)*, 1430.

(15) Hupfer, B.; Ringsdorf, H. Spreading and polymerization behavior of diacetylenic phospholipids at the gad-water interface. *Chem. Phys. Lipids* **1983**, *33*, 263.

(16) Heo, J.-M.; Son, Y.; Han, S.; Ro, H.-J; Jun, S.; Kundapur, U.; Noh, J.; Kim, J.-M. Thermochromic

polydiacetylene nanotube from amphiphilic macrocyclic diacetylene in aqueous solution. *Macromolecules* **2019**, *52*, 4405.

(17) Van den Heuvel, M.; Löwik, D. W. P. M.;Van den Hest, J. C. M. Self-assembly and polymerization of diacetylene-containing peptide amphiphiles in aqueous solution. *Biomacromolecules* **2008**, 7, 2727.

(18) Jahnke, E.; Weiss, J.; Neuhaus, S.; Hoheisel, T. N., Frauenrath, H. Synthesis of diacetylene-containing peptide building blocks and amphiphiles, their self-assembly and topochemical polymerization in organic solvents. *Chem. Eur. J.* **2009**, *15*, 388.

(19) Fuhrhop, J.-H., Blumtritt, P.; Lehmann, C.; Luger, P. Supramolecular assemblies, a crystal structure, and a polymer of N-diacetylenic gluconamides. *J. Am. Chem. Soc.* **1991**, *113*, 7437.

(20) Lorraine, H.; Cvetanovich, G. L.; Stupp, S. I. Peptide amphiphile nanofibers with conjugated polydiacetylene backbones in their core. *J. Am. Chem. Soc.* **2008**, *130*, 3892.

(21) Wang, G.; Goyal, N.; Mangunuru, H. P. R.; Yang, H.; Cheuk, S.; Narasimha Reddy, P. V. Preparation and self-assembly study of amphiphilic and bispolar diacetylene-containing glycolipids. *J. Org. Chem.* **2015**, *80*, 733.

(22) Zhong, L.; Zhu, X.; Duan, P.; Liu, M. Photopolymerization and formation of a stable purple Langmuir-blodgett film based on the gemini-typeamphiphilic diacetylene derivatives. *J. Phys. Chem. B* **2010**, *114*, 8871.

(23) Perino, A.; Schmutz, M.; Meunier, S.; Mésini, P. J.; Wagner, A. Self-assembled nanotubes and helical tapes from diacetylene nonionic amphiphiles, structural studies before and after polymerization. *Langmuir* **2011**, *27*, 12149.

(24) Huo, Q.; Russell, K. C.; Leblanc, R. M. Chromatic studies of a polymerizable diacetylene hydrogen bonding self-assembly: a "self folding" process to explain the chromatic changes of polydiacetylenes. *Langmuir* **1999**,15, 3972.

(25) Judge, M. D.; Lowen, S. V.; Holden, D. A. Synthesis and characterization of a novel amphiphilic polydiacetylene. *Macromolecules* **1991**, *24*, 3709.

(26) Ohba, S.; Engbersen, J. F. J. Synthesis of novel amphiphilic diacetylenes with amino or ammonium functionality. *Tetrahedron* **1991**, *47*, 9947.

(27) Tieke, B.; Weiss, K. Amphiphilic diacetylenes with pyridine and 2,2′-bipyridine headgroups – polymerization properties in the crystalline state, in LB-multilayers, and in complexes with transition metal salts. Morphology of polymerized multilayers. *Colloid Polym. Sci.* **1985**, *263*, 576.

(28) Tachibana, H.; Yamanaka, Y.; Sakai, H.; Abe, M.; Matsumoto, M. Effect of position of butadiyne moiety in amphiphilic diacetylenes on the polymerization in the Langmuir–Blodgett films. *Macromolecules* **1999**, *32 (25)*, 8306.

(29) van den Heuvel, M.; Löwik, D. W. P. M.; van Hest, J. C. M. Effect of the diacetylene position on the chromatic properties of polydiacetylenes from self-assembled peptide amphiphiles. *Biomacromolecules*, **2010**, *11(6)*, 1676.

(30) Okada, S.; Peng, S.; Spevak, W.; Charych, D. Color and chromism of polydiacetylene vesicles. *Acc. Chem. Res*. **1998**, *31(5)*, 229.

(31) Bunton, C.A.; Ionescu, L.G. Hydrolysis of di- and trisubstituted phosphate esters catalyzed by nucleophilic surfactants. *J. Am. Chem. Soc*, **1973**, *95 (9)*, 2912.

(32) Bowling, N.P.; Burrmann, N.J.; Halter, R.J.; Hodges, J.A.; McMahon, R.J. Synthesis of simple diynals, diynones, their hydrazones, and diazo compounds: precursors to a family of dialkynyl carbenes (R^1—C≡C—C¨C≡C—R^2). *J. Org. Chem.* **2010**, *75*, 6382.

(33) Bales, B. L.; Benrraou, M.; Zana, R. Krafft temperature and micelle ionization of aqueous solutions of cesium dodecyl sulfate. *J. Phys. Chem. B* **2002**, *106(35)*, 9033.

(34) Kalyanasundaram, K.; Thomas, J. K. Environmental effects on vibronic band intensities in pyrene monomer fluorescence and their application in studies of micellar systems. *J. Am. Chem. Soc.* **1977**, *99(7)*, 2039.

(35) Pons, M.; Foradada, M.; Estelrich, J. Liposomes obtained by the ethanol injection method. *Int. J. Pharm.* **1993**, *95(1-3),* 51

(36) Lapinski, M. M.; Castro-Forero, A.; Greiner, A. J.; Ofoli, R. Y.; Blanchard, G. J. Comparison of liposomes formed by sonication and extrusion: rotational and translational diffusion of an embedded chromophore. *Langmuir* **2007**, *23(23)*, 11677.

(37) Bayati, S.; Galantini, L.; Knudsen, K. D.; Schillén, K. Effects of Bile Salt Sodium Glycodeoxycholate on the Self-Assembly of PEO–PPO–PEO Triblock Copolymer P123 in Aqueous Solution. *Langmuir* **2015**, *31*, 13519.

(38) Belloni, L.; Drifford, M. On the Effect of Small Ions in the Dynamics of Polyelectrolyte Solutions. *J. Phys. Lett.* **1985**, 46, 1183.

(39) Missel, P.J.; Mazer, N. A.; Benedek, G. B.; Young, C. Y.; Carey M. C. Thermodynamic Analysis of the Growth of Sodium Dodecyl Sulfate Micelles *J. Phys. Chem.* **1980**, *84*, 1044.

(40) Fischer, M.; Schmölzer, C.; Nowikow, C.; Schmid, W. Indium-Mediated Allenylation of Aldehydes and Its Application in Carbohydrate Chemistry: Efficient Synthesis of D-Ribulose and 1-Deoxyun. 201-D-ribulose. *Eur. J. Org. Chem.* **2011**, *9*, 1645.

(41) Neuberg, P.; Perino, A.; Morin-Picardat, E.; Anton, N.; Darwich, Z.; Weltin, D.; Mely, Y.; Klymchenko, A. S.; Remy, J.-S.; Wagner, A. Photopolymerized micelles of diacetylene amphiphile: physical characterization and cell delivery properties. Chem. Commun. **2015**, *51*, 11595.

(42) Perino, A.; Klymchenko, A.; Morere, A.; Contal, E.; Rameau, A.; Guenet, J.-M.; Mély, Wagner, A. Structure and behavior of polydiacetylene-based micelles. *Macromol. Chem. Phys*. **2011**, *212*, 111.

(43) Moghaddam, B.; Habib Ali, M.; Wilkhu, J.; Kirby, D.J.; Mohammed, A. R.; Zheng, Q.; Perrie, Y. The application of monolayer studies in the understanding of liposomal formulations. *Int. J. Pharm.* **2011**, *417*, 235.

(44) Inglot, K.; Martyński, T.; Bauman, D. Influence of the alkyl chain length of some mesogenic molecules on their Langmuir film formation ability. *Liquid Crystals* **2006**, *33(7)*, 855.

(45) Hertmanowski, R.; Biadasz, A.; Martyński, T.; Bauman, D. Optical spectroscopy study of some 3,4,9,10-tetra-(n-alkoxycarbonyl)-perylenes in Langmuir–Blodgett films. *J. Mol. Struct.* **2003**, *646*, 25.

(46) Yu, Z.-W.; Jin, J.; Cao, Y. Characterization of the liquid-expanded to liquid- condensed phase transition of monolayers by means of compressibility. *Langmuir* **2002**, *18*, 4530.

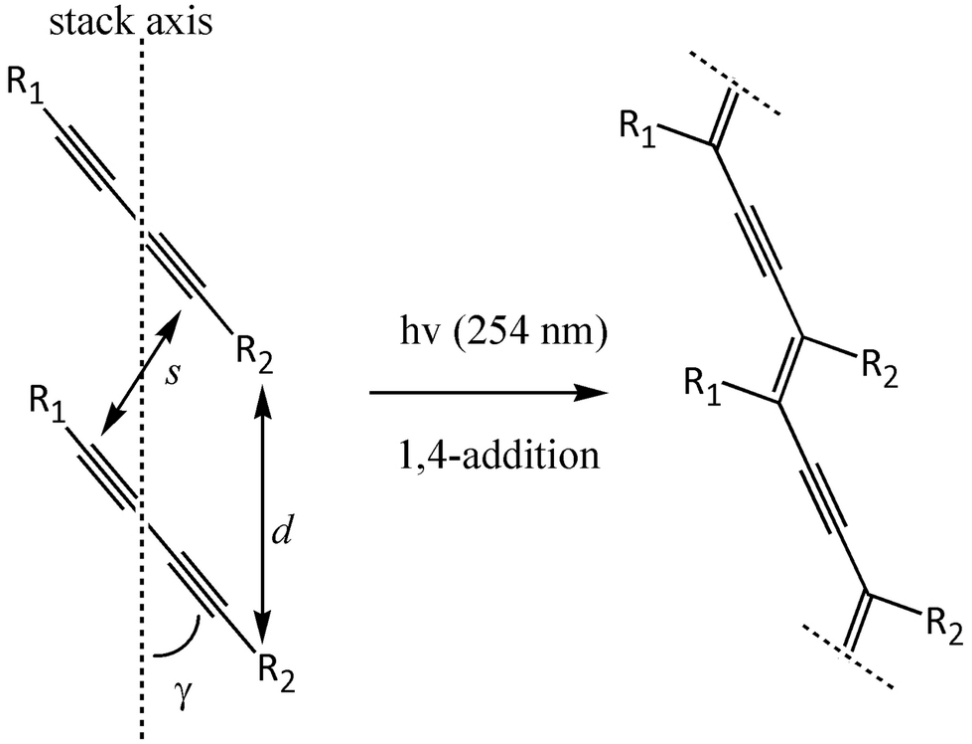

Scheme 1. Favourable geometric parameters of monomers in crystal lattice (d = 4.9 Å, s = 3.4 Å, γ ~ 45 °) for topochemical polymerization.

85x63mm (300 x 300 DPI)

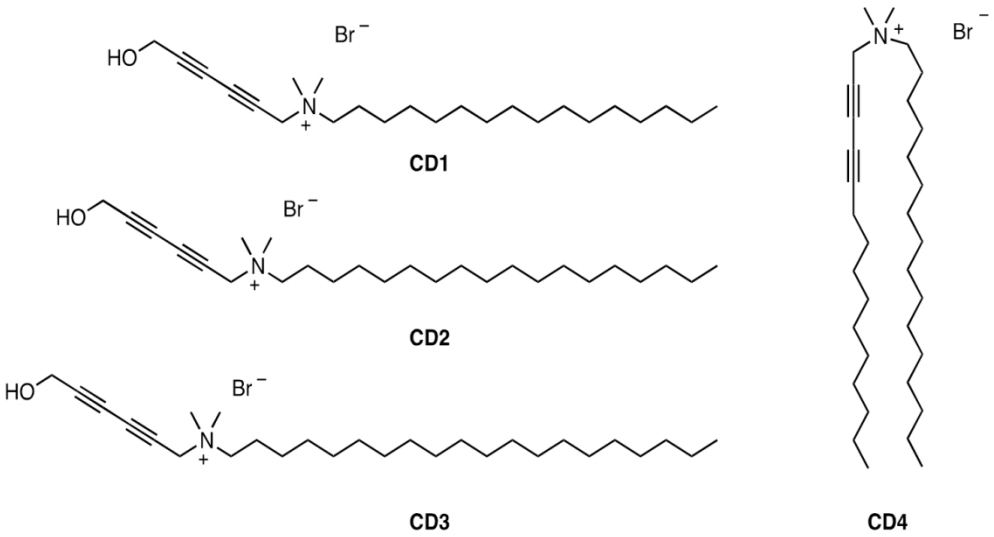

Chart 1. Molecular structures of the newly synthetized CDs 1-4.

85x45mm (440 x 440 DPI)

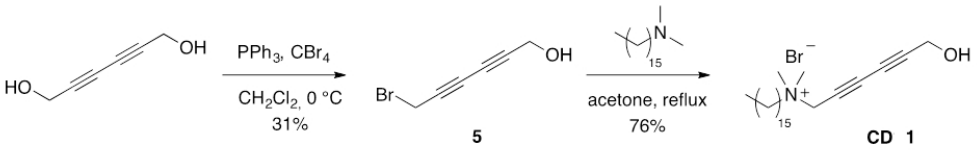

Scheme 2. Synthetic pathway to obtain amphiphile CD 1

84x15mm (287 x 287 DPI)

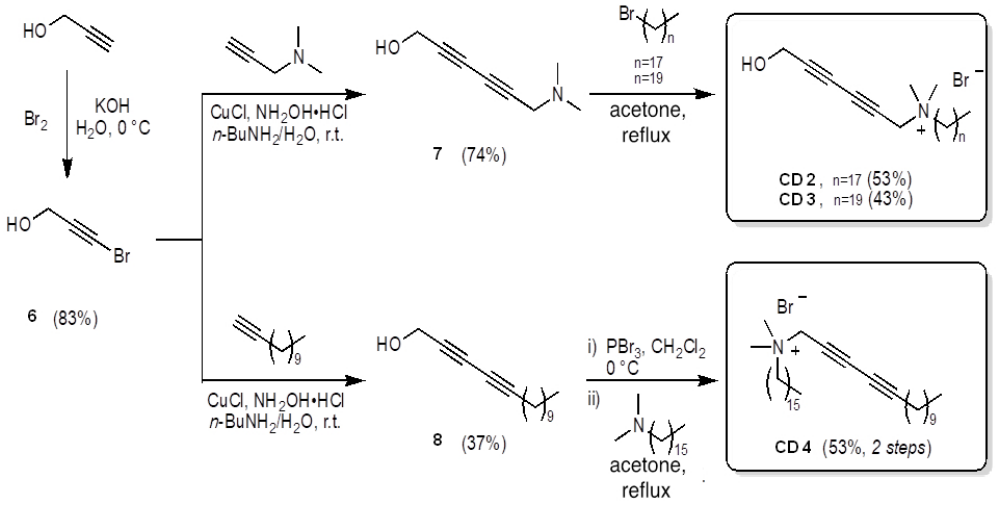

Scheme 3. Synthetic pathways to obtain amphiphiles CDs 2-4

84x43mm (287 x 287 DPI)

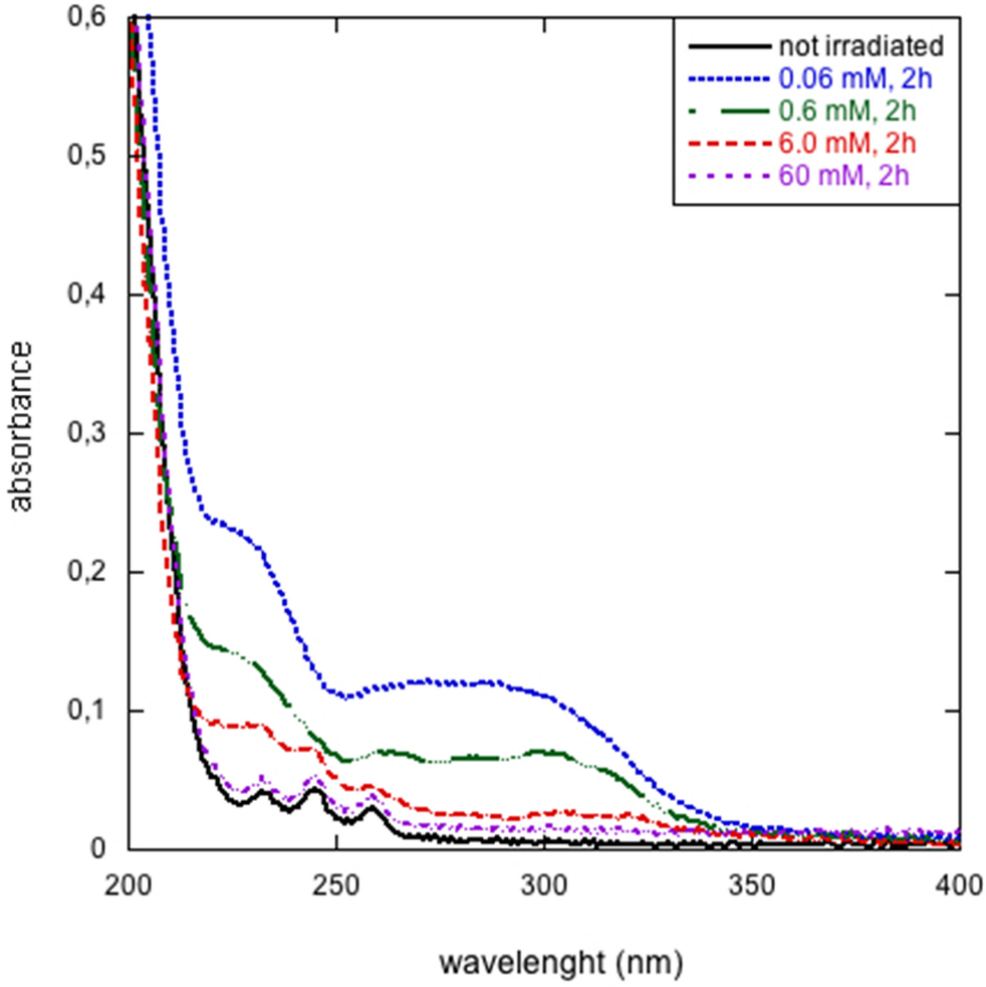

Figure 1. Absorption spectra of aqueous CD 1 solutions recorded after two hours of irradiation carried out at 60 °C and different concentrations: 0.06 (blue dotted trace), 0.6 (green dashed dotted trace), 6.0 (red dashed trace) and 60 (purple dashed trace) mM; black solid trace is referred to the non-irradiated sample 0.06 mM. An analogue behavior was observed in the case of CD 2 and CD 3.

84x84mm (300 x 300 DPI)

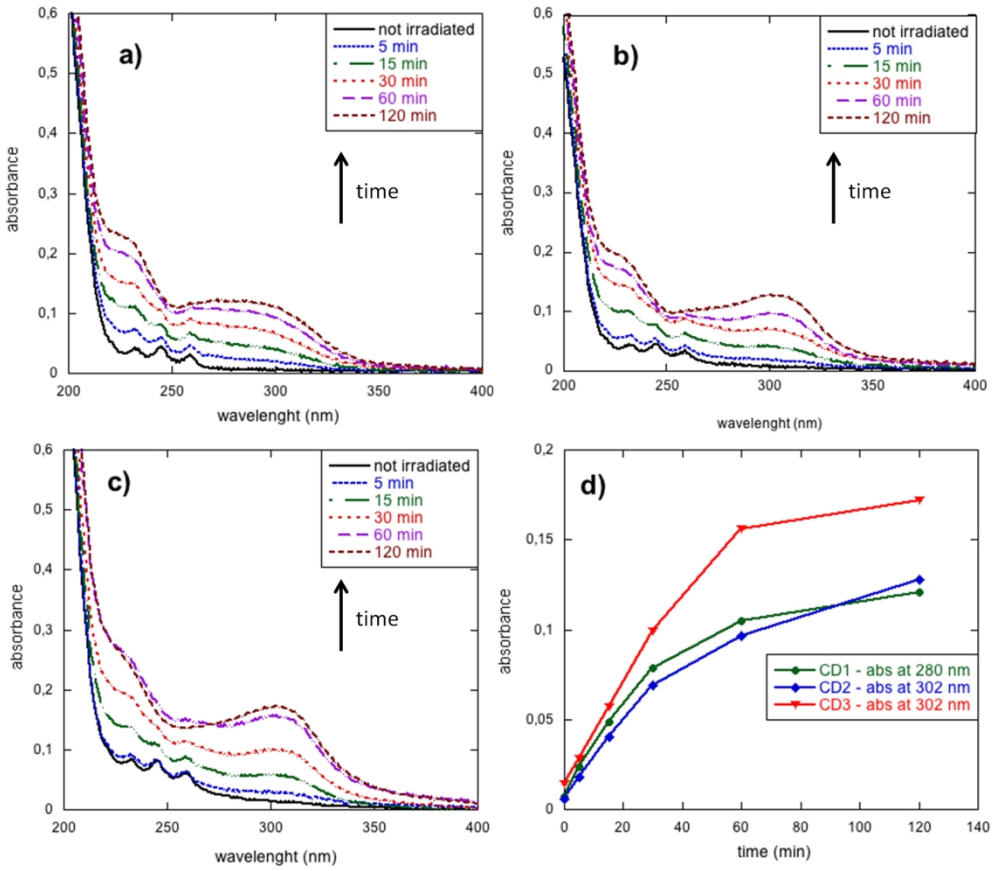

Figure 2. Absorption spectra of 0.06 mM aqueous solutions of a) CD1, b) CD2 and c) CD3 recorded at fixed times of irradiation at 60 °C; d) evolution of intensity of absorption maximum as a function of irradiation time.

174x153mm (300 x 300 DPI)

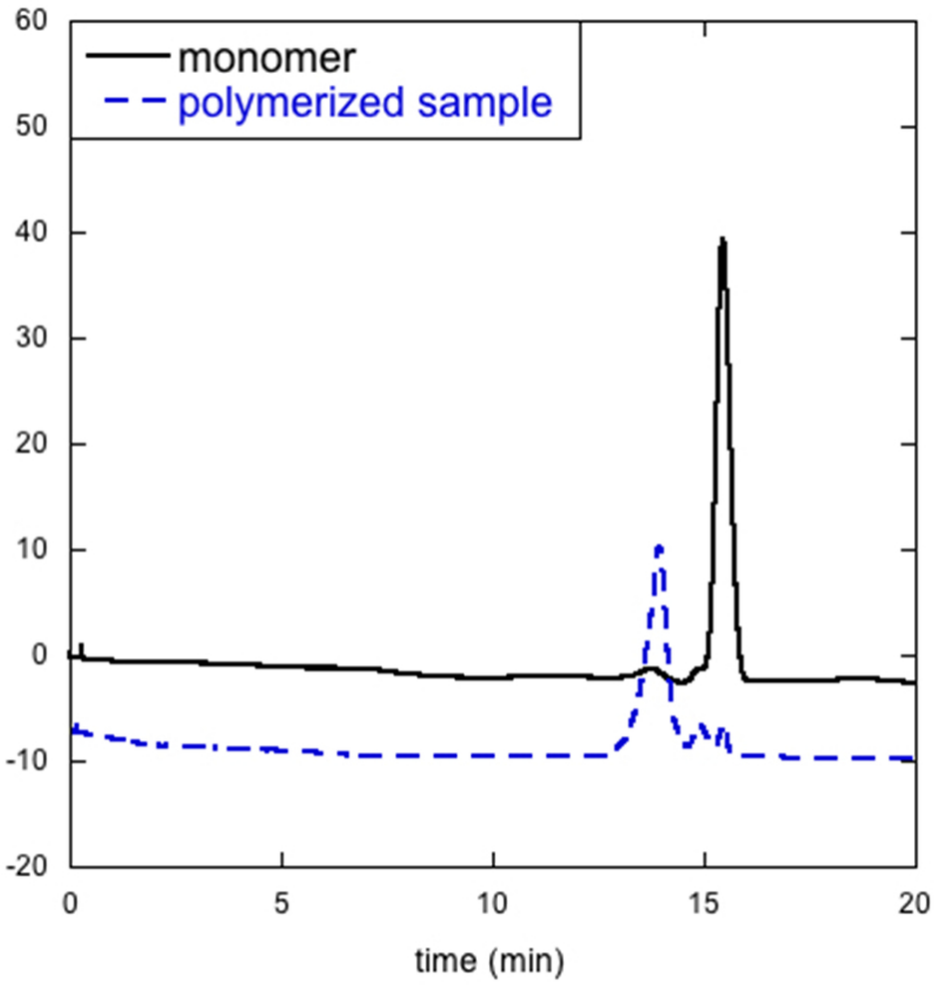

Figure 3. GPC chromatograms relative to monomeric (black solid trace) and polymerized (blue dashed trace) samples of CD 1 (eluent DMF with LiBr 0.1% w/w).

84x84mm (300 x 300 DPI)

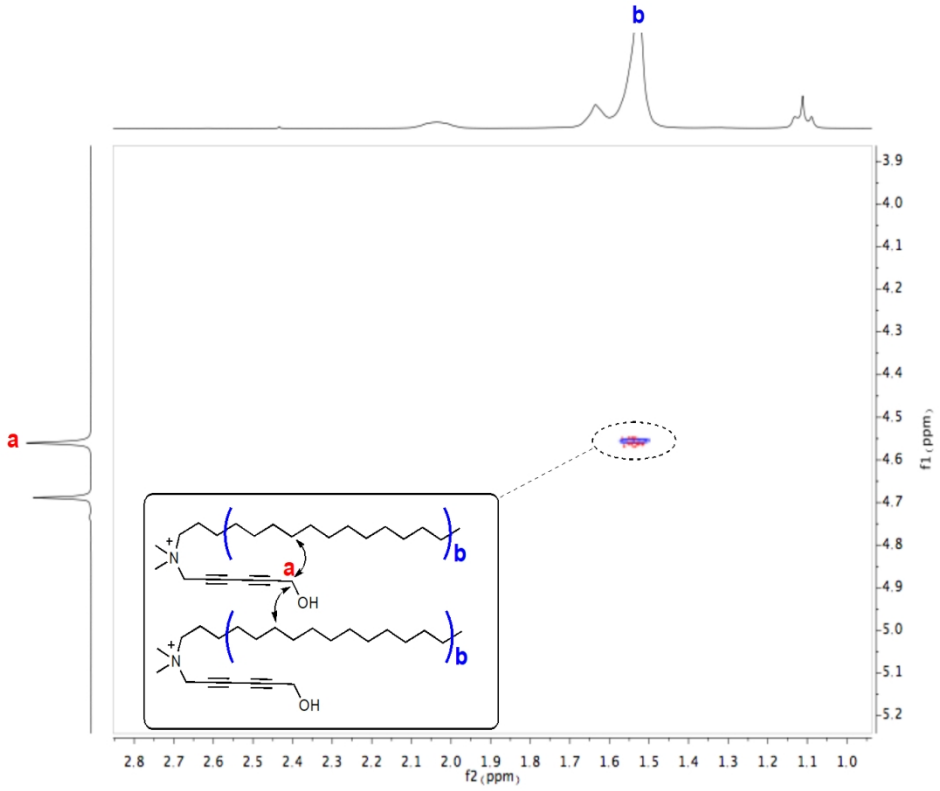

Figure 4. Region of ROESY spectrum of the 60 mM sample of CD1 in D2O and representation of the topology of amphiphiles within the aggregates; folding of hydroxyhexadiynyl group in the hydrophobic region of the micelle is consistent with the presence of the correlation peak between the methylene group adjacent to the hydroxyl group (4.46 ppm) and those of the hexadecyl chain.

85x67mm (440 x 440 DPI)

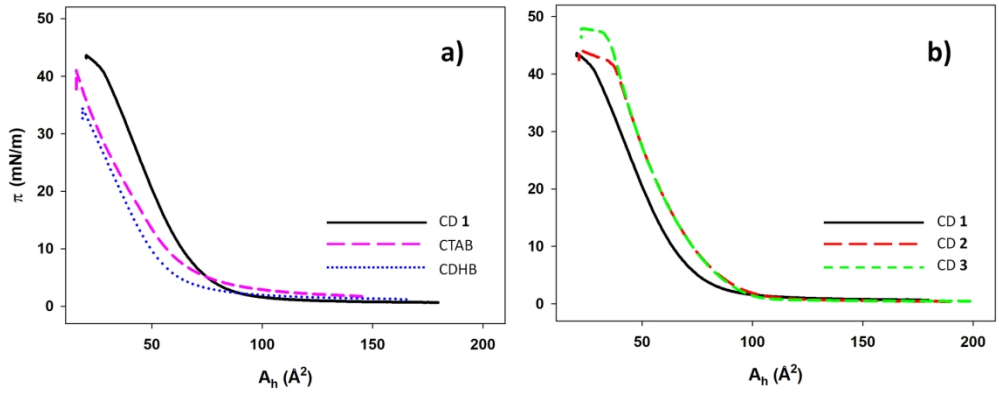

Figure 5. π−A isotherms of monolayers of CD 1 (black line in A and B) and A) CTAB (purple line), CDHB (blue line); B) CD 2 (red line) and CD 3 (green line) monolayers.

174x68mm (300 x 300 DPI)

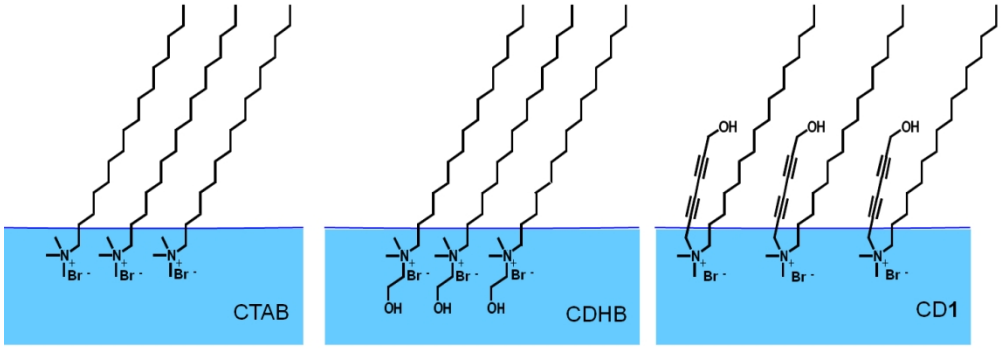

Figure 6. Schematic representation of CTAB and CDHB with the hydroxylethyl group protruding toward the subphase, and CD 1 monolayer with the diacetylenic segment folded toward the hydrophobic region.

85x32mm (440 x 440 DPI)

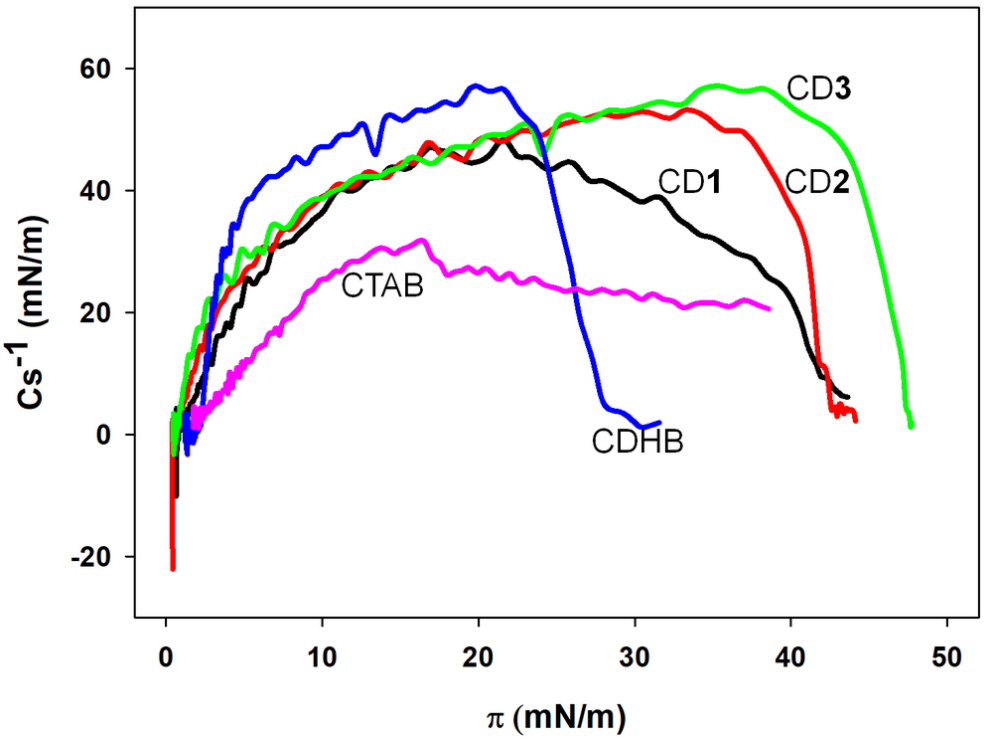

Figure 7. Compressibility modulus of CTAB (yellow line), CDHB (blue line), CD1 (purple line), CD2 (red line) and CD3 (green line) monolayers.

85x63mm (300 x 300 DPI)

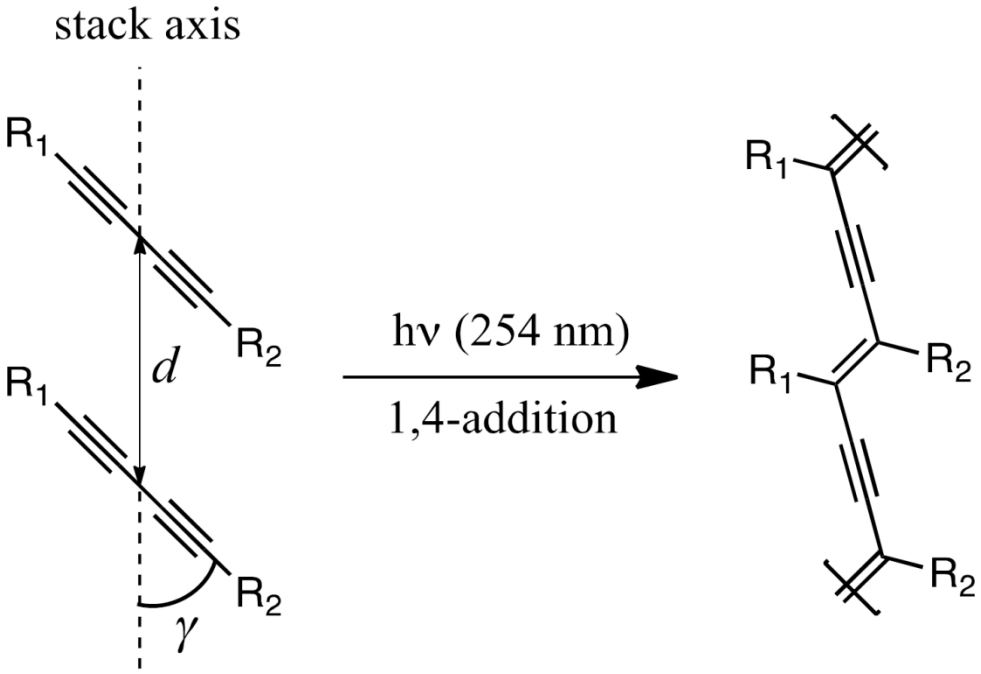

Scheme 4. Topology of diacetylenic residues for the polymerization of CD 1 within the aggregates. At concentrations not largely above the cmc, the loose structure of the aggregates could allow the appropriate alignment of diacetylene moieties for the occurrence of 1,4-addition. The folding of the hydroxyhexadiynyl toward the hydrophobic region of the micelle has been deduced from the ROESY and Langmuir through measurements.

389x269mm (96 x 96 DPI)

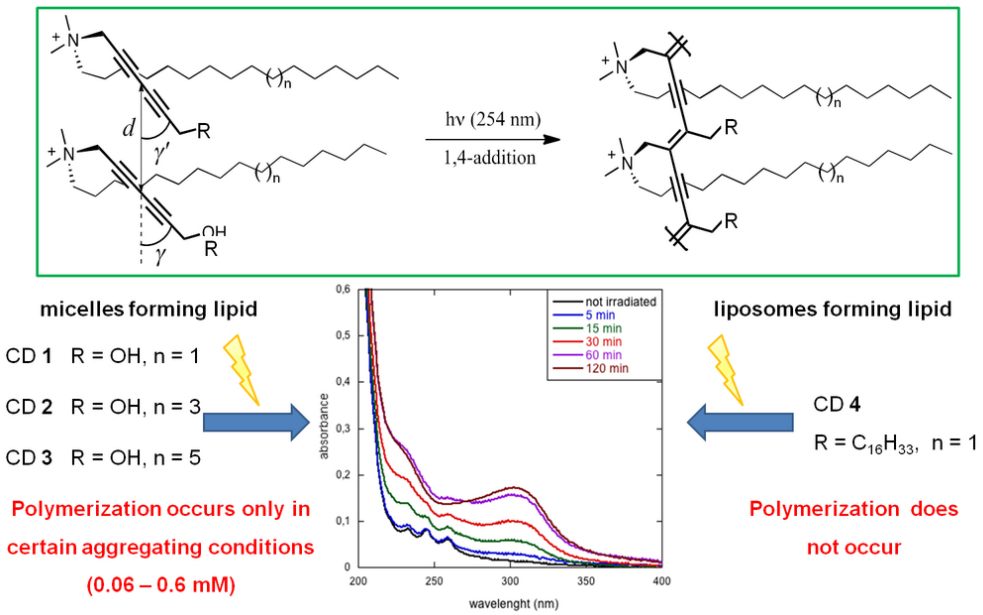

Table of Contents Graphic

85x53mm (300 x 300 DPI)